Development 136, 1539-1548 (2009) doi:10.1242/dev.032425

The mechanism and pattern of yolk consumption provide insight into embryonic nutrition in *Xenopus*

Paul Jorgensen[1], Judith A. J. Steen[2,3], Hanno Steen[3,4] and Marc W. Kirschner[1,*]

Little is known about how metabolism changes during development. For most animal embryos, yolk protein is a principal source of nutrition, particularly of essential amino acids. Within eggs, yolk is stored inside large organelles called yolk platelets (YPs). We have gained insight into embryonic nutrition in the African clawed frog *Xenopus laevis* by studying YPs. Amphibians follow the ancestral pattern in which all embryonic cells inherit YPs from the egg cytoplasm. These YPs are consumed intracellularly at some point during embryogenesis, but it was not known when, where or how yolk consumption occurs. We have identified the novel yolk protein Seryp by biochemical and mass spectrometric analyses of purified YPs. Within individual YPs, Seryp is degraded to completion earlier than the major yolk proteins, thereby providing a molecular marker for YPs engaged in yolk proteolysis. We demonstrate that yolk proteolysis is a quantal process in which a subset of dormant YPs within embryonic cells are reincorporated into the endocytic system and become terminal degradative compartments. Yolk consumption is amongst the earliest aspects of differentiation. The rate of yolk consumption is also highly tissue specific, suggesting that nutrition in early amphibian embryos is tissue autonomous. But yolk consumption does not appear to be triggered by embryonic cells declining to a critically small size. Frog embryos offer a promising platform for the in vivo analysis of metabolism.

KEY WORDS: Yolk, Cell size, Seryp, Vitellogenin, EP45, pNiXa, *Xenopus*

INTRODUCTION

For most animals, embryogenesis is an external process: they develop from eggs deposited directly into the environment. As they construct themselves, these embryos are limited to the resources contained within the egg. Therefore, externally developing embryos typically contain large reserves of lipid droplets, glycogen and yolk, which provide the energy and building blocks required for embryogenesis.

Yolk protein is the predominant source of essential amino acids for the embryo and provides many additional nutrients, including phospholipids, cholesterol and phosphate. Yolk is stored in dense, membrane-bound organelles called yolk platelets (YPs). These organelles appear to be highly conserved, as the YPs of animals in diverse phyla are formed by essentially the same mechanism and contain homologous proteins (Fischer et al., 1996; Grant and Hirsh, 1999; Hayakawa et al., 2006; Opresko et al., 1980; Roth and Porter, 1964). Yolk is consumed over the course of embryogenesis, but animals have evolved different ways of consuming it. The two main patterns, which need not be mutually exclusive, are: (1) organisms in which these YPs are distributed to all embryonic cells, which consume the yolk intracellularly (e.g. amphibians, sea urchins, the nematode *Caenorhabditis elegans*) and (2) organisms that develop a yolk sac to digest the YPs and the surrounding cytoplasm and to distribute nutrients to the embryo proper (e.g. birds, teleost fish, octopi, insects).

With a few notable exceptions (e.g. sea urchins, dipteran flies), the major yolk proteins in animals are derived from the large conserved lipoprotein Vitellogenin (Brooks and Wessel, 2002; Smolenaars et al., 2007). Vitellogenin is apparently never synthesized by the oocyte, but is extracted from maternal fluids upon binding to the highly conserved Vitellogenin receptor (Schneider, 1996). The maternal cell type that provides Vitellogenin differs in different phyla. Examples include the intestine in *C. elegans* (Kimble and Sharrock, 1983), the fat body in mosquitoes (Hagedorn et al., 1973) and the liver in vertebrates (Wahli et al., 1981). Once endocytosed, Vitellogenin is processed, often being partially proteolyzed into smaller proteins termed Vitellins or Lipovitellins and, in vertebrates, Phosvitins and Phosvettes (Romano et al., 2004). YPs are thought to be specialized late endosomes or lysosomes, that accumulate and then store the processed Vitellogenin (Fagotto, 1995; Grant and Hirsh, 1999).

In *X. laevis*, YPs occupy around half the volume of the egg, yet Vitellogenin derivatives account for ~90% (by weight) of egg protein (Gurdon and Wakefield, 1986). Such a density of Vitellogenin derivatives is possible because these proteins are stored in crystalline form within the YP. Vitellogenin derivatives largely suffice to feed the embryo, probably because Vitellogenin is highly nutritious. In addition to providing the essential amino acids within its ~1800 amino acid chain, Vitellogenin associates with ~50 lipid molecules, ~95 molecules of covalently bound phosphate, as well as about one zinc, two calcium, three magnesium, 0.5 iron and numerous sodium and potassium ions (Montorzi et al., 1995; Ohlendorf et al., 1977; Thompson and Banaszak, 2002; Wiley and Wallace, 1981).

We have gained fundamental insights into the mechanism of YP consumption, a poorly understood process that is likely to be conserved throughout the animal phyla. Our studies have further revealed that yolk consumption is an early aspect of differentiation and that there is a spatial and temporal pattern to nutrition in the *Xenopus* embryo.

MATERIALS AND METHODS

Molecular biology and chemicals

Standard molecular biology and *X. laevis* techniques were followed (Sambrook and Russell, 2001; Sive et al., 2000). Unless otherwise specified, chemicals and enzymes were from Sigma-Aldrich (St Louis, MO, USA).

[1]Department of Systems Biology, Harvard Medical School, Boston, MA 02115, USA. [2]F. M. Kirby Neurobiology Center, Children's Hospital Boston, and Department of Neurobiology, Harvard Medical School, Boston, MA 02115, USA. [3]Proteomics Center at Children's Hospital Boston, Boston, MA 02115, USA. [4]Department of Pathology, Harvard Medical School and Children's Hospital Boston, Boston, MA 02115, USA.

*Author for correspondence (e-mail: marc@hms.harvard.edu)

Accepted 2 March 2009

Purification of yolk platelets and proteomic analysis

Several hundred eggs were activated with the calcium ionophore A23187, resuspended in YP isolation buffer [YPIB: 20 mM HEPES-KOH pH 7.4, 50 mM KCl, 250 mM sucrose, 1 mM EDTA, 1 mM DTT, 1× Complete protease inhibitors (Roche, Basel, Switzerland), 100 μg/mL PMSF, 1 μM pepstatin], then lysed in a loose-fitting Dounce homogenizer. Lysate was layered onto a preformed Percoll gradient (ρ=1.12) and centrifuged (30,000 ***g***, 1 hour, 4°C). White, high-density (ρ≥1.15) bands were isolated and the high-density Percoll/organelle mixture was gently mixed and centrifuged again (20,000 ***g***, 4°C, 30 minutes) to yield two distinct white bands of YPs. To obtain YPs from tailbud embryos, several hundred embryos (stage 26) were placed in NKG dissociation buffer [100 mM sodium isethionate, 20 mM sodium pyrophosphate, 20 mM glucose, pH 9.0 (Newport and Kirschner, 1982)] with 0.05% benzocaine on a nutator at 4°C for 45 minutes. Single cells or small cell clusters were passed through a 70 μm cell strainer and were gently lysed in a loose-fitting Dounce homogenizer. YPs were then purified as above, but only a single density of YPs was observed. The bands of low-density egg YPs, high-density egg YPs and tailbud YPs were isolated and ultracentrifuged (130,000 ***g***, 4°C, 1 hour). Purified YPs were isolated from the top of the clear Percoll pellets and most were sonicated. These YP extracts were centrifuged (12,000 ***g***, 4°C, 10 minutes) to pellet YP crystals. This step removed >99% of the Vitellogenin derivatives Lipovitellin 1 (LV1) and Lipovitellin 2 (LV2). The 12,000 ***g*** supernatants were then ultracentrifuged (200,000 ***g***, 4°C, 1 hour) to pellet YP membranes (and any contaminating vesicles and organelles). The 200,000 ***g*** supernatants were isolated and concentrated in 10 kDa MWCO Centricon tubes (Millipore, Billerica, MA, USA).

The fractions were subjected to SDS-PAGE followed by staining with colloidal Coomassie (Invitrogen, Carlsbad, CA, USA). Bands of interest were excised and in-gel digested with trypsin. Peptides derived from in-gel digested proteins were analyzed by online microscale capillary reversed-phase HPLC hyphenated to a linear ion trap mass spectrometer (LTQ, Thermo Fisher Scientific, Waltham, MA, USA). Samples were loaded onto an in-house packed 100 μm i.d. × 15 cm C_{18} column (Magic C_{18}, 5 μm, 200 Å, Michrom Bioresources, Auburn, CA, USA) and separated at ~500 nL/minute with 30-minute linear gradients from 5 to 40% acetonitrile in 0.4% formic acid. After each survey spectrum the six most intense ions per cycle were selected for fragmentation/sequencing. All MS datasets were searched against a combined *X. laevis* and *X. tropicalis* RefSeq protein sequence database (September 2005, 16994 sequence entries) using the Mascot search engine (Matrix Science, v. 2.1.04, Boston, MA, USA). Peptides were identified with a Mascot score no less than 33 (P<0.05) and proteins were identified based on at least two unique peptides. Pro-Q Phosphoprotein Stain (Invitrogen) was detected with a Typhoon Trio instrument (GE Healthcare, Chalfont St Giles, UK). Coomassie staining and western blotting were imaged with an Odyssey Infrared Imager (Licor, Lincoln, NE, USA). The same western blot was sequentially probed with different primary antibodies, but the same fluorescent secondary antibody (goat anti-rabbit-Alexa680, Invitrogen A21109) was used for each round of detection.

Antibodies, sectioning and immunostaining

Polyclonal antibodies from rabbit were prepared (Covance, Princeton, NJ, USA) against Vitellogenin derivatives (anti-Vtg) and against Seryp (anti-Seryp). The immunogen for anti-Vtg was YP crystals (see above). The immunogen for anti-Seryp was purified inclusion bodies of untagged Seryp from *Escherichia coli*. IgG antibodies were purified from each rabbit serum and labeled with fluorophores (Invitrogen). Embryos at different stages were fixed in freshly prepared MEMFA (Sive et al., 2000), dehydrated and embedded in Paraplast. Sections (10 μm) were rehydrated, microwaved to promote antigen recovery, probed with anti-Vtg-Alexa488 and anti-Seryp-Alexa568, and *z*-series separated by 0.3 μm in ~30 steps obtained with confocal microscopy using a 100× Plan Apo NA 1.4 objective lens, TE2000U inverted microscope (Nikon, Melville, NY, USA), CSU10 spinning disk (Yokogawa, Tokyo, Japan), 3W Innova 70C Spectrum laser (Coherent, Santa Clara, CA, USA) and Orca-ER CCD camera (Hamamatsu, Bridgewater, NJ, USA). For quantitation, YPs were defined as ≥1 μm bodies, the periphery of which was stained with anti-Vtg. The percentage of YPs that completely lacked Seryp staining (Seryp$^-$) was determined. Each tissue at each stage was measured in at least three embryos derived from different females. The number of YPs counted depended on the size of the tissue and the YP density, but all the YPs in a selected region were counted. The number of counts ranged from 41 to 704 YPs/tissue, with a median of 134 YPs/tissue/embryo.

Dextran injection and tissue dissection

Late blastulae (stage 9) were twice injected in the blastocoel with 10 nL of 10 mg/mL fixable dextran-Alexa647 (10 kDa, Invitrogen). After developing to tailbud (stage 26), embryos were transferred to an agarose-coated dish containing 1×MMR with 0.05% benzocaine and 1 mg/mL collagenase. Extirpated tissues were transferred into NKG dissociation buffer (see above) in agarose-coated dishes. Dissociated cells were allowed to settle onto poly-D-lysine-coated coverslips for 15-45 minutes before being fixed in freshly prepared MEMFA and processed for immunostaining with anti-Vtg-Alexa488 and anti-Seryp-Alexa568.

Hydroxyurea/aphidicolin (HU/APH) treatment and CycA2/^{myc6}Cdk2 overexpression

Embryos just beginning gastrulation (stage 10-10.5) were incubated with 20 mM hydroxyurea (HU)/150 μM aphidicolin (APH)/0.5% DMSO or with 0.5% DMSO. After developing at 22°C for 11.5-12 hours (stage 17-20), embryos were fixed in MEMFA and the percentage of Seryp$^-$ YPs (as above) and the nuclear density (and hence average cell volume) in the prosencephalon (n=9 embryos from multiple females) were determined from sagittal sections. For 6/9 embryos, neighboring sagittal sections from the same embryo (within 200 μm) were stained with anti-phospho-Histone H3 (serine 10) (Millipore, 06-570), goat anti-rabbit-Alexa568 (Invitrogen, A11011) and DAPI to determine the mitotic index in the prosencephalon. Approximately 600 nuclei were counted (always more than 200) from up to six sections from the same embryo. To avoid double counting of nuclei, every other 10 μm section was quantitated. Capped transcripts encoding *X. laevis* Cyclin A2 (CycA2) and Cdk2 (with an N-terminal 6myc tag, ^{myc6}Cdk2) were prepared with mMESSAGE Machine (Ambion/Applied Biosystems, Austin, TX, USA). For each transcript, 250 pg was injected into the animal pole of both blastomeres at the two-cell stage. Injection of these transcripts had variable, clutch-dependent effects, including widespread embryo death and gastrulation defects. Presented data are derived from clutches in which the majority of injected embryos developed to late neurula (stages 18-19). Fixed embryos (n=8 embryos from multiple females) were sectioned such that neighboring transverse sections (always within 200 μm) from the same embryo could be probed to determine the percentage of Seryp$^-$ YPs, nuclear density and the mitotic index (as above). Anti-myc tag antibody (9E10, Santa Cruz Biotechnology, Santa Cruz, CA, USA, sc-40) and either goat anti-mouse-Alexa488 or goat anti-mouse-Alexa647 (Invitrogen A11001, A31625) identified cells expressing ^{myc6}Cdk2 for quantification.

RESULTS

The yolk platelet proteome

Because gradients of YP concentration and size form along the animal-vegetal axis during oogenesis (Danilchik and Gerhart, 1987), different embryonic lineages contain different numbers and sizes of YPs. Therefore, monitoring YP consumption in different embryonic tissues, by tracking YP numbers or size distributions over time, seemed insensitive and impractical (Robertson, 1978). However, we reasoned that the structure of the YP might allow us to distinguish dormant YPs from those that were engaged in active proteolysis. As in many amphibians and basal vertebrates, the YPs of *X. laevis* are composed of a limiting membrane, a central crystal of Vitellogenin derivatives and an intervening superficial layer of unknown composition (Karasaki, 1963; Romano et al., 2004). Therefore, if YPs were converted into active degradation compartments during development (Fagotto, 1995), components of the superficial layer would be degraded to completion prior to the crystalline core, as proteases would be likely to only have access to the outer surface of

the protein crystal. Electron microscopy (EM) has revealed that YPs lacking a superficial layer become increasingly abundant during amphibian development (Karasaki, 1963).

In order to discover novel YP components, we characterized the proteome of the *X. laevis* YP. The crystalline core of Vitellogenin derivatives has been characterized in *X. laevis* (Ohlendorf et al., 1977; Wiley and Wallace, 1981). During oogenesis, endocytosed Vitellogenin is partially proteolyzed into ~115 kDa Lipovitellin 1 (LV1), ~31 kDa Lipovitellin 2 (LV2), ~35 kDa Phosvitin (PHO), ~19 kDa Phosvette 1 (PVT1) and ~13 kDa Phosvette 2 (PVT2). PVT1 and PVT2 approximate to a cleaved PHO protein and may be derived from a particular isoform of Vitellogenin (Ohlendorf et al., 1977; Wahli et al., 1981; Wiley and Wallace, 1981). YPs were purified from frog eggs by isopycnic centrifugation, taking advantage of the very high density of the organelle. The purified YPs were disrupted by sonication, and differential centrifugation was used to separate YP crystals and other insoluble protein from the soluble proteins in the superficial layer (YP supernatant fraction) and proteins in the limiting membrane (YP membrane fraction). Our purification scheme removed most Vitellogenin derivatives, which allowed other YP proteins to be visualized and then identified by peptide sequencing in a mass spectrometer (see Fig. S1 and Table S1 in the supplementary material).

A number of plasma and lysosomal proteins were identified. Of interest, we identified the *X. laevis* homolog of Paraoxonase, a serum protein that protects the lipids of the low-density lipoprotein (LDL) from oxidation in mammals (Getz and Reardon, 2004). Intriguingly, the central protein component of LDL is apoB100, a lipoprotein that is evolutionarily related to Vitellogenin (Smolenaars et al., 2007). Amongst the lysosomal proteins, we identified two different aminopeptidases, as well as three hydrolases anticipated to attack glycosyl chains. No additional lysosomal proteases (e.g. Cathepsin D) were found, even though many of these proteases were represented in the queried sequence databases. Numerous proteins from the endoplasmic reticulum were identified, in particular protein disulfide isomerases, as well as many mitochondrial proteins. Additional tests are required to determine whether these proteins represent contaminants or bona fide YP proteins.

Aside from Vitellogenin, the most frequently identified peptides originated from a protein that we have named Seryp (serpin in the yolk platelet). Previously named EP45 and pNiXa, Seryp is a female-specific serum protein that, like Vitellogenin, is induced by estrogen and secreted from the liver in *X. laevis* (Beck et al., 1992; Holland et al., 1992). Seryp is a member of the antitrypsin-like subfamily of the serpin superfamily (Irving et al., 2000). Consistently, Seryp has been shown to covalently complex with, and non-competitively inhibit, bovine chymotrypsin in vitro (Kotyza et al., 1998). Although identified in oocytes and embryos, its subcellular location has never been made clear (Sunderman et al., 1996). BLAST searches reveal that Seryp is not a well-conserved protein, being most closely related to two serpins from *X. tropicalis* (44% identity over more than 370 amino acids) and to another serpin from *X. laevis* (39% identity over more than 360 amino acids) that

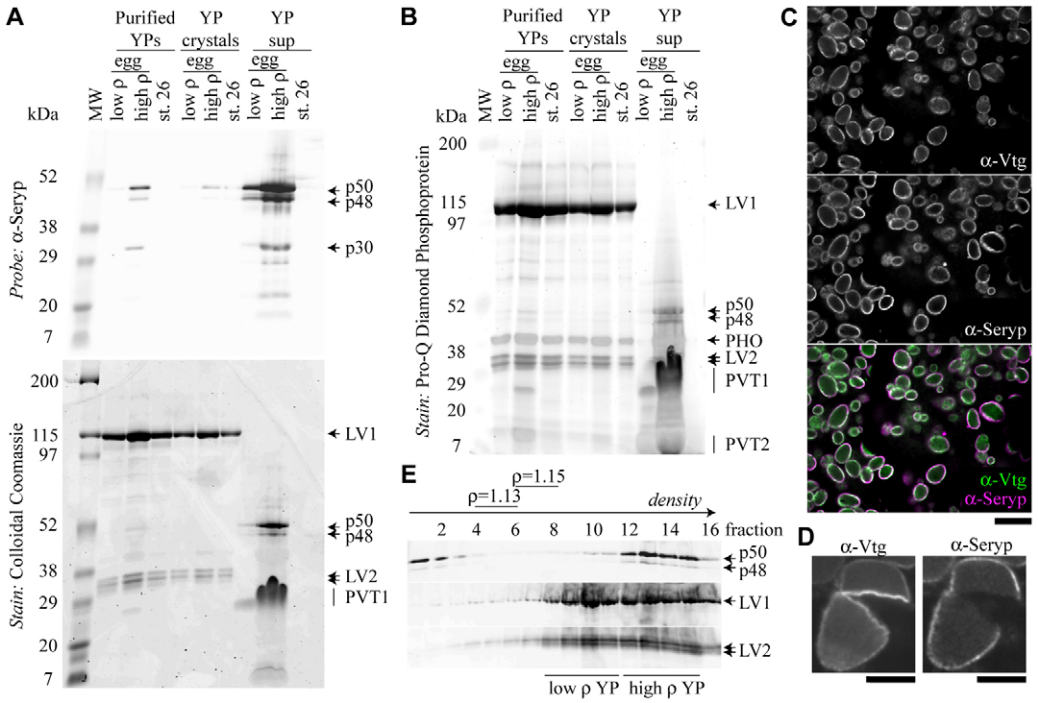

Fig. 1. Seryp is a novel component of the YP superficial layer. (**A**,**B**) YPs were purified from eggs [low and high density (ρ) YPs] and tailbud stage embryos (stage 26) and the contents subfractionated into YP crystal and YP supernatant (sup) fractions. Purified YPs and the two derived fractions were analyzed by western blotting (A), Coomassie staining (A) and phosphoprotein staining (B). Seryp species were greatly enriched in the YP supernatant fraction, whereas LV1 and LV2 were nearly exclusively in YP crystals. The phosphoprotein stain identified PHO, PVT1 and PVT2, based on approximate size similarity to the major yolk phosphoproteins described by Wiley and Wallace (Wiley and Wallace, 1981). PVT1 also stained with Coomassie and appeared to migrate anomalously when greatly enriched in the YP supernatant. (**C**,**D**) Anti-Vtg-Alexa488 (α-Vtg) and anti-Seryp-Alexa568 (α-Seryp) antibodies colocalize to the rim of YPs in unfertilized egg sections (C). Anti-Vtg-Alexa488 but not anti-Seryp-Alexa568 bound to the interior of YP crystals that cracked during sectioning (D). Scale bars: 10 μm in C; 5 μm in D. (**E**) When subjected to isopycnic centrifugation, gently lysed single eggs exhibited lower density, low Seryp YPs and higher density, high Seryp YPs, as well as Seryp that did not sediment. Fractions that contained ρ=1.13 and ρ=1.15 density markers are indicated. Smearing on the western blots was likely to be due to Percoll in the gel wells.

was not identified in our YP proteomic study. It is therefore unclear whether Seryp has been recently recruited to the YP in the *X. laevis* lineage or if antitrypsin-like serpins are conserved YP components.

Seryp is a novel constituent of the yolk platelet superficial layer

Polyclonal antibodies were raised against Vitellogenin derivatives (anti-Vtg) and against Seryp (anti-Seryp). We purified and then biochemically dissected YPs from eggs and from tailbud embryos (stage 26) (Fig. 1A,B). In eggs, but not tailbud embryos, we consistently observed two distinct populations of YPs that differed in density, as previously observed (Jared et al., 1973; Neff et al., 1984). Anti-Vtg identified LV1 and LV2, but could not detect the highly phosphorylated PHO, PVT1 and PVT2. These latter proteins were visualized to varying degrees with either a Coomassie or a phosphoprotein stain (Fig. 1A,B). Anti-Seryp identified three species (p50, p48, p30) that were greatly enriched in the supernatant fraction of purified YPs that had been disrupted by sonication. p50 is the most abundant form and has the predicted molecular weight of Seryp; p48 and p30 are presumably products of partial proteolysis. By this biochemical analysis, Seryp and PVT1 appear to be the most abundant soluble proteins in the YP and, as such, are presumably located in the YP superficial layer.

To confirm the localization of Seryp to the YP superficial layer, sections were cut from unfertilized eggs and immunostained (Fig. 1C). Anti-Vtg and anti-Seryp colocalized to YP rims (98%, n=3 eggs, >1450 YPs). Anti-Vtg antibodies apparently could not penetrate the crystalline YP core. But sectioning frequently cracked YPs, exposing the interior of the YP crystal to antibodies. In such cracked YPs, anti-Vtg invariably stained the natural edge of the YP as well as the cracked edge of the crystal (Fig. 1D). By contrast, anti-Seryp only stained the natural edge of the YP, confirming that Seryp is not found within the crystalline core of the YP and is limited to the superficial layer.

Tailbud embryo YPs and the lower density egg YPs mostly lacked proteins in the YP supernatant fraction (Seryp, PVT1), but did contain proteins from the YP crystal fraction (LV1, LV2, PHO) (Fig. 1A,B). Curiously, nearly all egg YPs were Vtg$^+$ and Seryp$^+$ by immunostaining, and subsequent experiments revealed that many YPs in tailbud embryos still contain Seryp (see below). To determine if lower density YPs might be derived from a subset of eggs, single eggs were gently lysed and subjected to isopycnic density fractionation. Single eggs had lower and higher density YPs (Fig. 1E). Seryp was present in the denser YPs, but it was also found at the very top of the density gradient where soluble, cytoplasmic proteins would be found. Immunostaining never revealed substantial Seryp outside of YPs (Fig. 1C). These observations can be reconciled by concluding that some aspect of the lysis or density gradient centrifugation causes a substantial number of egg YPs and all tailbud YPs to lose their limiting membrane (Wallace and Karasaki, 1963). During development, YPs may become closely associated with cytoskeletal elements (Selchow and Winklbauer, 1997), which might tear the YP membrane during lysis of the embryonic cells, leading to a complete failure to obtain intact YPs from tailbud embryos.

Seryp enters the oocyte with Vitellogenin

We wondered whether Seryp, like Vitellogenin, might be a maternal somatic product that is not synthesized in the oocyte. Given that both Seryp and Vitellogenin are estrogen-responsive serum proteins that are secreted from the liver (Holland et al., 1992), it seemed plausible that Seryp also entered YPs by endocytosis during oogenesis. We prepared extracts of staged oocytes (Fig. 2A). Egg forms of Seryp (p50, p48, p30) were always present in later oocyte stages (III-VI, 15 of 15). Strikingly, in the earliest stages (I,II), oocytes did not always contain the standard forms of Seryp but did contain a novel protein (p60) detected by our anti-Seryp antibody. p60 was present in all stage I and II oocytes (5 of 5) and in most stage III oocytes (3 of 4). p60 abundance in later stage oocytes (IV-VI) was more variable (see Fig. S2 in the supplementary material).

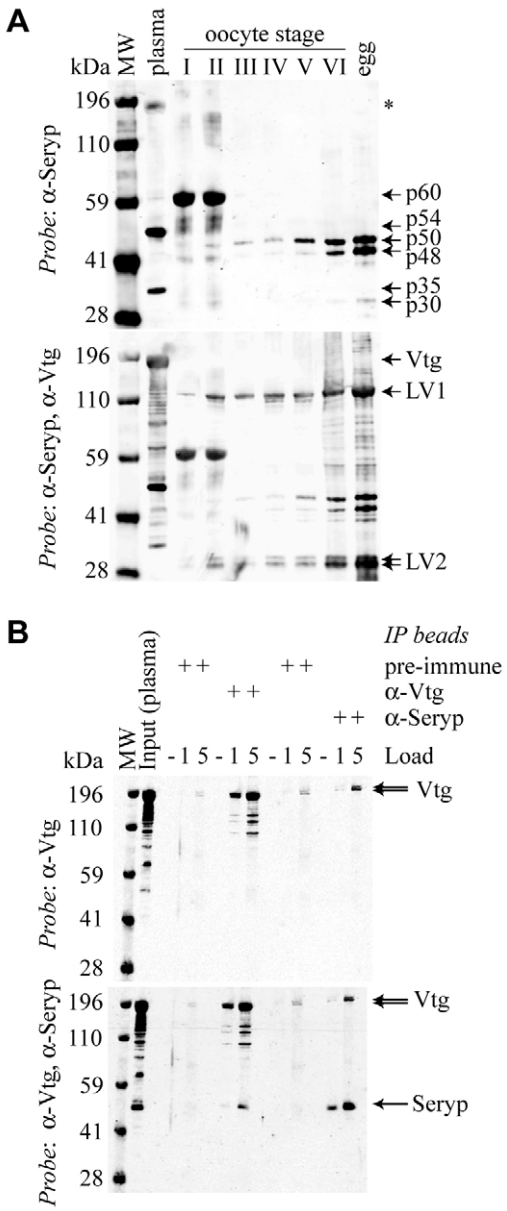

Fig. 2. Seryp is taken up by oocytes from plasma, probably through interaction with Vitellogenin. (**A**) Seryp species have different electrophoretic mobilities. Female *X. laevis* plasma contains a 54 kDa Seryp species, the precursor of the egg forms p50 and p48. Early oocytes contain a ~60 kDa protein that cross-reacts strongly with anti-Seryp antibody. Asterisk indicates cross-reaction with highly abundant serum Vitellogenin. Gel loading was approximately normalized by oocyte volume. (**B**) Reciprocal co-immunoprecipitation of Vitellogenin and Seryp from female *X. laevis* plasma. Antibody cross-linked beads were prepared from IgG purified from pre-immune and immunized anti-Vtg rabbit serum, as well as from pre-immune and immunized anti-Seryp rabbit serum. Western blots were sequentially probed with anti-Vtg and anti-Seryp antibodies.

In reciprocal co-immunoprecipitation experiments, Seryp and Vitellogenin interacted in *X. laevis* plasma (Fig. 2B), as originally suggested by ultracentrifugation experiments (Holland and Wangh, 1987). Minor yolk proteins in chicken interact with the Vitellogenin receptor, accounting for their concentration in the yolk (Jacobsen et al., 1995). Interaction with Vitellogenin may be an additional mechanism for targeting proteins to the YP. As Seryp is far less abundant in plasma than Vitellogenin (more than 50-fold molar difference, data not shown), only a fraction of the Vitellogenin entering the oocyte need interact with Seryp to account for the abundance of Seryp in oocytes and eggs.

Using qRT-PCR, we did not detect *SERYP* transcripts in oocytes of any stage or in embryos at several stages (see Fig. S3 in the supplementary material). Spiking in vitro transcribed *SERYP* transcripts into RNA preparations from embryos demonstrated that the sensitivity of the assay would be sufficient to detect ~1 transcript per typical metazoan cell or ~100,000 transcripts per frog oocyte, egg or embryo. Using this number as the maximal possible amount of *SERYP* transcript present in oocytes or eggs, simple calculations show that Seryp translation in oocytes and eggs, if any, is insignificant relative to the massive accumulation and degradation of this protein (~1 μg per egg) during oogenesis and embryogenesis, respectively. We conclude that, like Vitellogenin, Seryp is a maternal somatic protein that is endocytosed and stored by oocytes and then consumed during embryogenesis.

Seryp is eliminated from embryos and from individual YPs prior to Vitellogenin derivatives

Although the bulk of Vitellogenin derivatives and Seryp were not degraded until late in embryogenesis, Seryp species clearly declined prior to the Vitellogenin derivatives in whole embryos (Fig. 3A,B), as previously suggested (Grbac-Ivankovic et al., 1994). Variability in the absolute YP protein content of *X. laevis* eggs (Fig. 3B), and the fact that most of the yolk protein is concentrated in the presumptive gut (Hausen and Riebesell, 1991), precluded using bulk measurements of Seryp and Vitellogenin derivatives as a useful indicator of yolk consumption.

As described above, we suspected that within individual YPs a superficial-layer protein like Seryp would be degraded prior to the central crystal of Vitellogenin derivatives. Indeed, in some tissues of tailbud embryos, many YPs completely lacked Seryp ($Seryp^{-}$) but did contain Vitellogenin derivatives (Vtg^{+}) (Fig. 3C). As essentially all egg YPs stained positive for Seryp (Fig. 1C), yolk proteolysis had apparently initiated in these tissues.

Yolk platelets that lack Seryp have been reincorporated into the endocytic system in a quantal fashion

There is no consensus on how yolk is proteolyzed intracellularly. In the most cited current model, it is argued that in *X. laevis* and many other species YPs need only be acidified to activate preloaded proteases (Fagotto, 1995). This model was based on observations that YPs become more acidic during development in many organisms and protease activities can be found in dormant YPs. In an alternative model, YPs would be activated by fusion with endosomes or lysosomes. The increased acidity of active YPs would be a secondary consequence of endocytic proton pumps, and not an independent regulatory step. The entire repertoire of lysosomal hydrolases and transporters would then be available to hydrolyze the diverse substrates present in the YP (see Introduction) and to export small molecules. Previously, in newt embryos, endocytosed ferritin was observed by EM in YPs that appeared to be in the process of degradation (Komazaki and Hiruma, 1999).

To test the endosome fusion model, we injected fixable dextran conjugated to a fluorescent dye into the blastocoel (i.e. extracellular space) of late blastulae (stage 9). The embryos were reared to tailbud stage (stage 26), select tissues dissected and cells dissociated. Endocytosed dextran had accumulated in a subset of

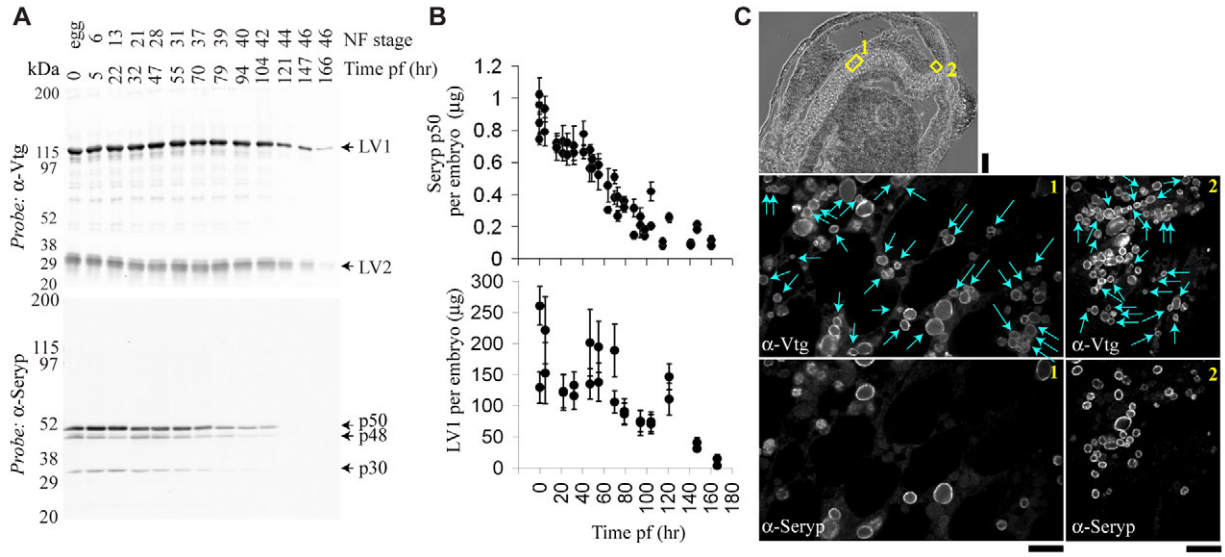

Fig. 3. Seryp is proteolyzed prior to Vitellogenin. (**A**) By bulk measurement (western blotting), Vitellogenin derivatives (LV1, LV2) and Seryp species (p50, p48, p30) decline at later stages of development. Extracts are ordered by time post-fertilization (pf) and Nieuwkoop-Faber stage (NF). Load: 1/500 (top blot) or 1/50 (bottom blot) of single embryos. (**B**) Quantitative dot blotting of extracts prepared from single embryos confirms that Seryp is consumed prior to Vitellogenin during development. Absolute levels of LV1 and Seryp p50 were obtained from standard curves relating antibody binding (fluorescence intensity) to absolute amounts of each protein. Each dot is the average for a single embryo ±1 s.d. (**C**) Seryp could not be detected in many YPs in tailbud embryos. Notochord (1) and prosencephalon (2) (yellow boxes) from a sagittal section of a tailbud embryo (top, stage 26, scale bar: 100 μm) were immunostained with anti-Vtg and anti-Seryp and imaged by confocal microscopy (bottom, scale bars: 10 μm). Blue arrows highlight YPs without detectable Seryp.

YPs in many cells (Fig. 4A,B). Of the dextran$^+$ bodies larger than ~1 μm (n=349 from 149 cells), 91% were Vtg$^+$ YPs. Strikingly, only 3% of these dextran-positive bodies were Seryp$^+$. There were still many Vtg$^+$ Seryp$^+$ YPs present in these cells (Fig. 4A,B). In short, the subsets of Vtg$^+$ YPs that were dextran$^+$ and Seryp$^+$ were nearly mutually exclusive. The data argue that the subset of YPs that are engaged in proteolysis have also been mixing with compartments of the endocytic system. We will refer to this subset of YPs as being 'activated'. Since they accumulate most of the dextran present in the cell (Fig. 4A,B), activated YPs appear to be the principal terminal degradative compartments in frog embryonic cells. As single cells from a variety of tissues contained both activated and dormant YPs (Fig. 4C), YP proteolysis is, per platelet, a quantal process within embryonic cells.

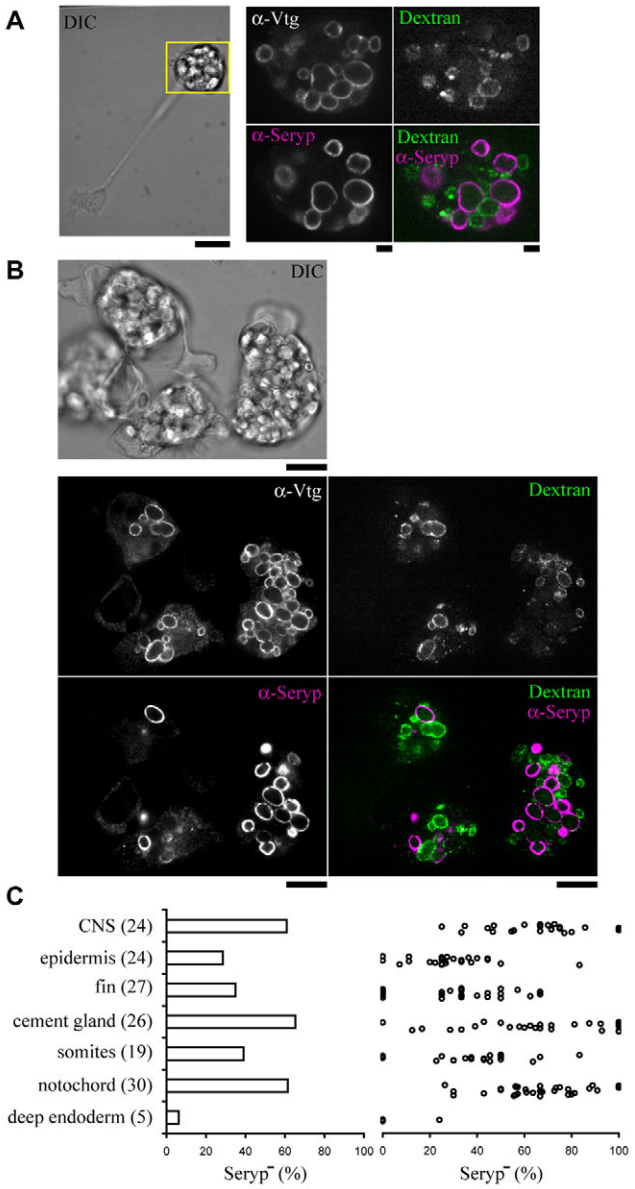

Fig. 4. Activated YPs have been reincorporated into the endocytic system. (**A**,**B**) YPs containing Seryp were almost mutually exclusive with YPs that accumulated extracellular dextran. Embryonic tissues were dissected from a tailbud embryo (stage 26) that had been previously injected in the blastocoel at the late blastula stage with fluorescently labeled, fixable dextran-Alexa647. The cells in the dissected tissues were dissociated and were immunostained with anti-Vtg and anti-Seryp. A neuron (A) and notochord cells (B) are presented. The soma of the neuron, boxed in yellow in the left panel, is further magnified in the right panels. Scale bars: 10 μm in A (left), B; 2 μm in A (right). (**C**) The average percentage of Seryp$^-$ YPs (left) and the percentage of Seryp$^-$ YPs in individual cells (right) was plotted for seven different dissociated tissues. The number of cells quantified is in brackets.

The dorsal lineages of the early neurula are actively consuming yolk

Using the absence of Seryp as a marker of YP activation, we characterized yolk consumption during frog embryogenesis. An atlas of YP activation during early embryonic development was generated (Fig. 5A,B). We immunostained sections from eggs and from six early embryonic stages: blastula (stage 9), gastrula (stage 12), early neurula (stage 14), late neurula (stage 18), early tailbud (stage 21) and tailbud (stages 26-27). Prominent tissues in each embryonic stage were imaged by confocal microscopy and the percentage of YPs (Vtg$^+$) that completely lacked any Seryp staining (Seryp$^-$) was determined (see Table S2 in the supplementary material).

Several tissues in early neurulae were avidly consuming yolk (Fig. 5C). Although it avoids the perils of quantitating fluorescence, our binary YP classification has an inherent delay, namely the time to degrade Seryp to completion. Therefore, it is not possible to say when YP consumption is first initiated. A previous histological survey concluded that YP consumption commences much later in embryogenesis, starting in the tailbud stages (Selman and Pawsey, 1965). By contrast, there have been scattered reports of YP breakdown prior to the tailbud stages in various amphibians (Fagotto and Maxfield, 1994; Karasaki, 1963; Komazaki et al., 2002; Robertson, 1978). Our results provide a conclusive demonstration that yolk consumption occurs throughout nearly the whole of *X. laevis* embryogenesis.

Activated YPs generally correlated with morphological differentiation. Ectodermal cells and the dorsal mesodermal cells differentiate in structure during neurulation, when the percentage of activated YPs abruptly rises. Among ectodermal tissues, the prosencephalon and eye had the highest percentages of activated YPs. Induction of the cement gland and lens from epidermis correlated with increased YP consumption (Fig. 5A,B). Morphological changes to the endoderm first occur in tailbud embryos, when the visceral pouches form during stages 23-27 (Nieuwkoop and Faber, 1994). Consistently, marked YP consumption took place in the arch and oral endodermal epithelium of tailbud embryos (stage 27), but not in morphologically static deep endoderm (Fig. 5A,B).

Most YP protein is, however, inherited by the deep endoderm that develops into the gut. Degradation of the bulk of Seryp and Vitellogenin derivatives accompanies gut development during the later tailbud and tadpole stages (Fig. 3A,B). It has been thought that the YPs of the gut are degraded extracellularly, by digestion of yolky cells within the intestinal lumen (Gerhart, 1980; Hausen and Riebesell, 1991). However, recent fate maps suggest that all deep endoderm cells are incorporated into the intestinal wall (Chalmers and Slack, 2000). Cells of the developing intestine wall, in fact, contained numerous intracellular, activated YPs (see Fig. S4 in the supplementary material). Therefore, even in the developing gut, yolk consumption was intracellular and correlated with morphological differentiation.

The onset of yolk consumption is not triggered by small cell size

Our survey of YP activation indicated that something happens between the blastula and early neurula stages to trigger this process, particularly in the neurectoderm. In the blastula, animal pole cells, which will give rise to the neurectoderm, are relatively small owing to previous asymmetric animal-vegetal divisions. The neurectoderm is also the most actively dividing tissue in early neurulae (Saka and Smith, 2001). Neurectoderm cells are therefore likely to be the smallest in the neurula and these cells also exhibit the largest

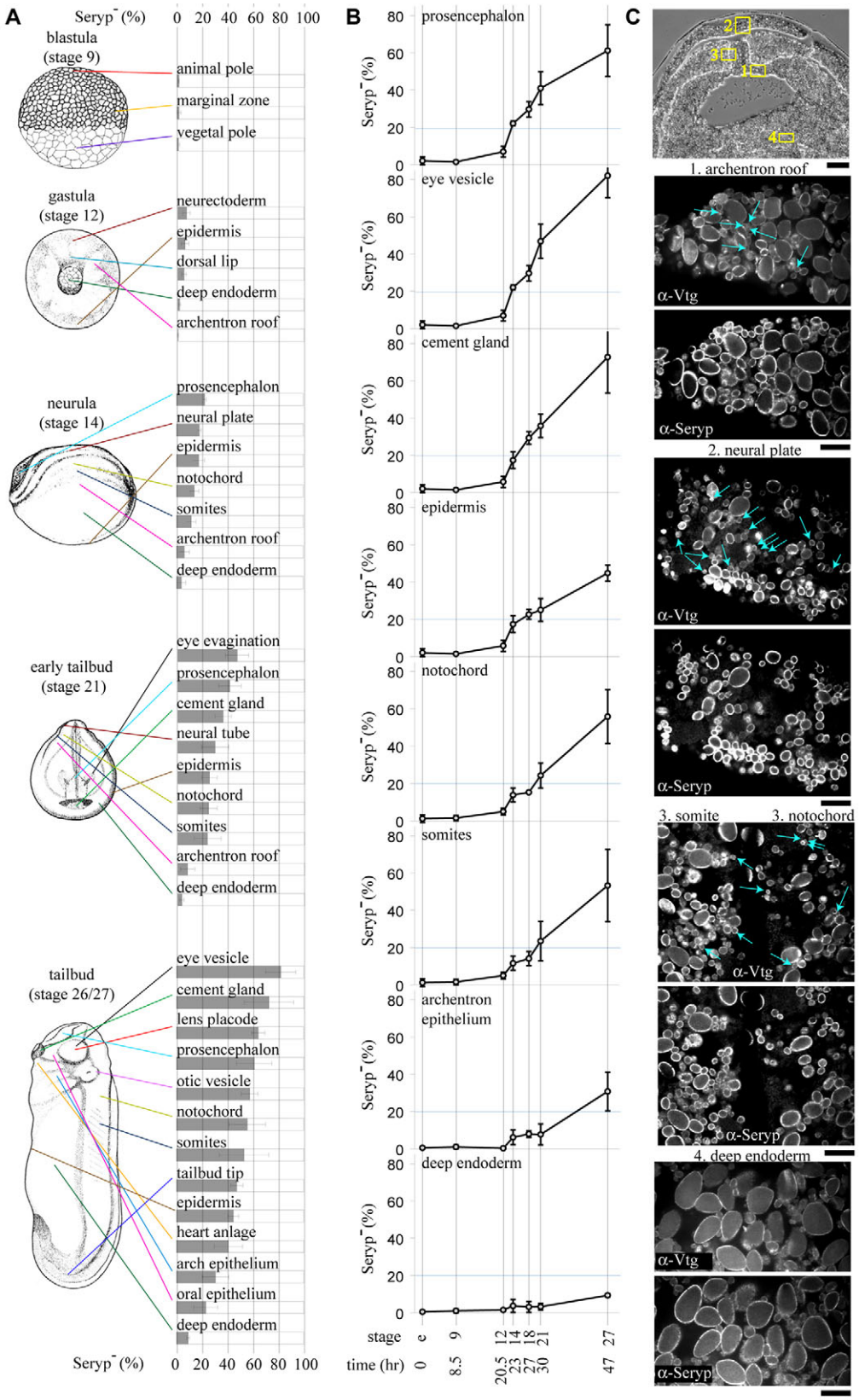

Fig. 5. An atlas of YP consumption during early frog embryogenesis. (**A**) The percentage of Seryp⁻ YPs in each of the tissues and stages depicted, as well as from unfertilized eggs and mid-neurulae (stage 17/18), was quantified. See supplementary material Table S2 for all numbers. For illustrative purposes, tissues (most of which are strictly internal) are approximately located on drawings (Nieuwkoop and Faber, 1994). The average ±1 s.d. of at least three embryos descended from different female frogs is presented. (**B**) Seryp⁻ (%) was plotted, using the most relevant tissues present at each stage. For instance, somites at stage 27 were most related to the somitogenic mesoderm at stage 14, to the dorsal lip at stage 12, and to the marginal zone of stage 9 embryos and eggs. (**C**) Activated YPs that have no detectable Seryp are apparent in multiple tissues in early neurulae (blue arrows). A transverse section of an early neurula (top, scale bar: 100 μm) locates tissues (yellow boxes) immunostained with anti-Vtg and anti-Seryp and imaged by confocal microscopy (bottom, scale bars: 10 μm).

percentage of active YPs (Fig. 5). We considered the possibility that small cell size induces compensatory cell growth and hence YP consumption.

Exposing early gastrula embryos to the DNA replication inhibitors hydroxyurea (HU) and aphidicolin (APH) blocks the cell cycle, but allows normal neurula development (Hardcastle and Papalopulu, 2000; Harris and Hartenstein, 1991). HU/APH-treated embryos had oversized cells, but degraded YPs as rapidly as control siblings (Fig. 6A,C-E). We performed the inverse experiment by generating undersized cells (Richard-Parpaillon et al., 2004). Cells expressing exogenous CycA2 and ^{myc6}Cdk2 (myc+) (Fig. 6B) displayed both a higher frequency of mitotic cells and a significant decrease in average cell size (~15%) (Fig. 6B-D), demonstrating that CycA2/^{myc6}Cdk2 was driving cell cycle progression and not just prolonging mitosis (den Elzen and Pines, 2001). Despite excessive cell cycle progression and small cell size, CycA2/^{myc6}Cdk2-expressing cells were not engaged in more rapid YP consumption (Fig. 6E).

DISCUSSION

Our results suggest a new general model for intracellular yolk consumption in embryonic cells. YP breakdown is a per-platelet quantal process within embryonic cells. In response to unknown developmental cues, individual YPs are somehow selected to begin fusing with endocytic compartments. Fusion with these compartments lowers the pH (Fagotto and Maxfield, 1994), allows extracellular dextran (Fig. 4) and ferritin access to the YP (Komazaki and Hiruma, 1999) and leads to the proteolysis of Seryp and, eventually, the crystal of Vitellogenin derivatives. In addition to proteases, phosphatases and other hydrolases, fusion events with late endosomes or lysosomes would supply lipid, amino acid and ion transporters.

The quantal mechanism of YP consumption appears to provide cells with a valve to control the rate of nutrient release. If cells did not single out a subset of YPs, but instead activated all YPs simultaneously, several problems would be immediately apparent. The endocytic system would first need to cope with a rapid expansion in volume. Even if rapidly increasing the size of the endocytic system were not a problem, it is not clear how nutrient release would be controlled in such a scenario. To control nutrient release, this hypothetical cell could conceivably regulate the number of hydrolases provided to all of the YPs. By contrast, real embryonic cells appear to have a much simpler regulatory system. YPs are individually activated, perhaps at a rate controlled by intracellular nutrient sensors, and then degraded to completion.

The striking spatial differences in yolk consumption argues that nutrition in early frog embryos is tissue- and/or cell-autonomous. That is, tissues that differentiate early, such as the neural lineages and the somites, have a requirement for components of the YP and they obtain these components intracellularly, with cells in that tissue perhaps sharing nutrients through gap junctions. An alternative possibility, which our evidence does not support, was that all cells in the early embryo would simultaneously begin degrading yolk and sharing nutrients through the extracellular space. In later stage tailbud embryos, the developing vasculature may allow for an embryo-wide integration of nutrition (heart beating begins at stage

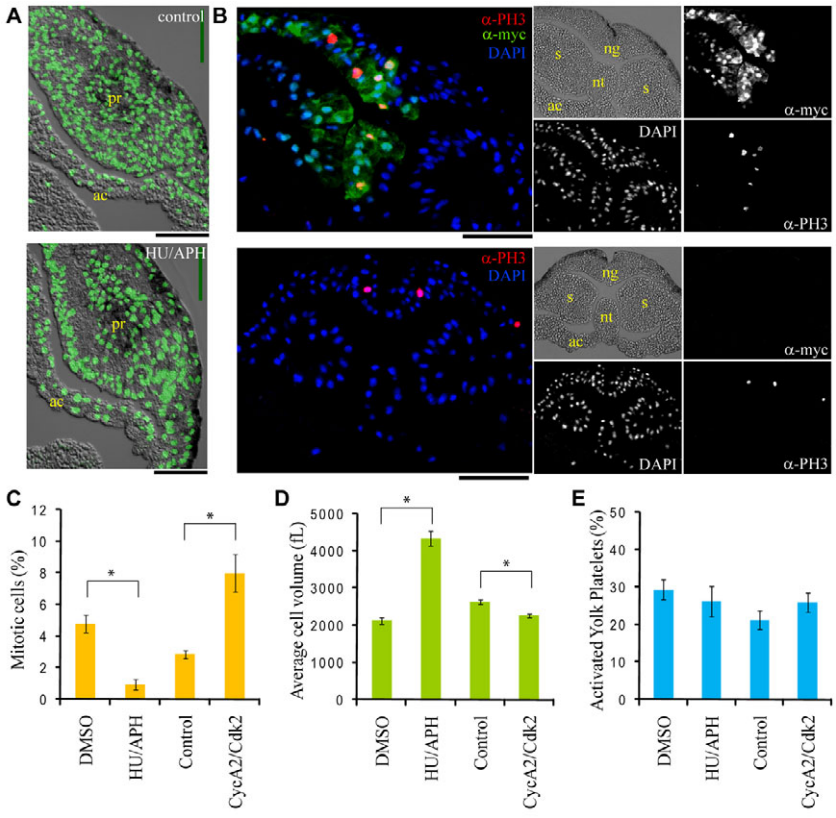

Fig. 6. Declining cell size during development does not induce YP activation. (**A**) Large cell size was apparent as decreased nuclear density (DAPI, green) in the prosencephalon of a late neurula treated with hydroxyurea/aphidicolin (HU/APH; bottom), as compared with control siblings (top). Scale bar: 100 μm. (**B**) Overexpression of CycA2 and ^{6myc}Cdk2 increased the frequency of mitotic cells in multiple lineages of late neurulae (top, uninjected control in bottom panels). Transcripts encoding the two proteins were injected into the animal pole at the two-cell stage. Cells expressing ^{6myc}Cdk2 were identified with anti-myc 9E10 antibody (α-myc), mitotic nuclei by anti-phospho-Histone H3 antibody (α-PH3). Right, single channel images; left, merged images. In contrast to a previous report (Richard-Parpaillon et al., 2004), CycA2/^{myc6}Cdk2 increased the mitotic index of the somitogenic mesoderm and of the normally postmitotic notochord (notochord, 7.4% versus 0%; somitogenic mesoderm, 5.2% versus 1.0% mitotic index; injected versus uninjected, n>160 cells). Scale bar: 100 μm. (**C-E**) The effects of HU/APH treatment and CycA2/^{6myc}Cdk2 overexpression on mitotic index, cell size and YP activation were quantified. HU/APH and DMSO control data are derived from the prosencephalon of late neurulae (stage 17-20), whereas CycA2/^{6myc}Cdk2 overexpression and uninjected control data are derived from the neural tube of late neurulae (stage 18-19). The average ±1 s.e. is presented. For HU/APH and DMSO control, n=9 embryos for cell size and YP activation and n=6 embryos for mitotic index. For CycA2/^{6myc}Cdk2 overexpression and uninjected control, n=8 embryos for all parameters. *P<0.01, Student's t-test. pr, prosencephalon; ac, archentron ceiling; ng, neural groove; nt, notochord; s, somitogenic mesoderm.

33-34). The vegetal mass (presumptive amphibian gut) inherits most of the yolk protein and yet comes to represent a proportionally smaller part of the embryo during the tadpole stages (Nieuwkoop and Faber, 1994). Nutrients released by intracellular breakdown of YPs within the cells of the gut are presumably exported into the blood and taken up by growing tissues during these later stages of embryogenesis.

Why do differentiating tissues consume yolk? This question is complicated by the fact that yolk consumption will release many different substances: not just amino acids, but cholesterol, phospholipids, fatty acids, phosphate and numerous positively charged ions. Differentiation per se requires no net synthesis of proteins: extant proteins can be degraded to allow for the remodeling of the proteome. But differentiation will certainly require energy, perhaps more energy than is required to maintain a cell that is not differentiating. Although it is often thought that yolk is consumed to provide energy, most evidence from early frog embryos argues against this. Free amino acids may provide some energy during the cleavage stages (Dworkin and Dworkin-Rastl, 1991) but, starting at gastrulation, the respiratory quotient and lack of ammonia production suggest that most respiration is driven by carbohydrate, and not amino acid, oxidation (Boell, 1948). Indeed, the frog egg has extensive energetic stores: ~5% of the dry mass of amphibian eggs is glycogen, and triacylglycerides are packed into abundant lipid droplets (Billett and Gould, 1971; Dworkin and Dworkin-Rastl, 1991; Hausen and Riebesell, 1991).

We argue that YP consumption in some tissues could signify a specialized form of growth, in which stored yolk protein is converted into the functional biomass of the embryo, such as cytoplasm and extracellular matrix. Growth has rarely been considered in such terms. Some might reasonably insist that growth can only be defined as an increase in total mass. But frog embryos clearly increase in volume (Tuft, 1962) (even when large extracellular spaces like the archentron are accounted for), synthesize new ribosomes (Baum and Wormington, 1985; Pierandrei-Amaldi et al., 1982) and accumulate large amounts of non-yolk proteins (see Fig. S5 in the supplementary material). Furthermore, few would dispute that chick embryos grow at the expense of their extra-embryonic yolk supply. The intracellular location of the yolk in amphibians (and many other organisms) does not change the fact that it is essentially a food that provides for growth of the embryonic tissues. It remains to be determined whether the canonical growth control pathways of somatic cells, such as the TOR pathway, control yolk consumption.

Aside from its small size (~1 mm) and amenability to biochemical, chemical, genetic and genomics approaches, the cell-autonomous nature of nutrition in early *X. laevis* embryos offers pleasing simplifications. Small molecule or genetic perturbations that incidentally cripple the nervous system, gut, or vasculature will block nutrition in feeding animals, but will not necessarily do so in frog embryonic cells laden with YPs, lipid droplets and glycogen. Future work in frog embryos might inform many aspects of metabolism in the embryonic and adult stages of vertebrate life.

We thank Lene Holland for providing expression constructs for Seryp/EP45; Anna Philpott for CycA2 and ^{myc6}Cdk2 expression constructs; Jennifer Waters and Lara Petrak of the Nikon Imaging Center at Harvard Medical School; as well as Justine Melo, Gary Ruvkun, Mike Springer, Jenny Gallop, Javier Apfeld, Chris Wylie, Janet Heasman and Brian Frederick for helpful discussions. P.J. is a Fellow of The Jane Coffin Childs Memorial Fund for Medical Research. This work was supported by NIH grant HD37277. Deposited in PMC for release after 12 months.

Supplementary material

Supplementary material for this article is available at http://dev.biologists.org/cgi/content/full/136/9/1539/DC1

References

Baum, E. Z. and Wormington, W. M. (1985). Coordinate expression of ribosomal protein genes during *Xenopus* development. *Dev. Biol.* **111**, 488-498.

Beck, B. L., Henjum, D. C., Antonijczuk, K., Zaharia, O., Korza, G., Ozols, J., Hopfer, S. M., Barber, A. M. and Sunderman, F. W., Jr (1992). pNiXa, a Ni(2+)-binding protein in *Xenopus* oocytes and embryos, shows identity to Ep45, an estrogen-regulated hepatic serpin. *Res. Commun. Chem. Pathol. Pharmacol.* **77**, 3-16.

Billett, F. S. and Gould, R. P. (1971). Fine structural changes in the differentiating epidermis of *Xenopus laevis* embryos. *J. Anat.* **108**, 465-480.

Boell, E. J. (1948). Biochemical differentiation during amphibian development. *Ann. NY Acad. Sci.* **49**, 773-800.

Brooks, J. M. and Wessel, G. M. (2002). The major yolk protein in sea urchins is a transferrin-like, iron binding protein. *Dev. Biol.* **245**, 1-12.

Chalmers, A. D. and Slack, J. M. (2000). The *Xenopus* tadpole gut: fate maps and morphogenetic movements. *Development* **127**, 381-392.

Danilchik, M. V. and Gerhart, J. C. (1987). Differentiation of the animal-vegetal axis in *Xenopus laevis* oocytes. I. Polarized intracellular translocation of platelets establishes the yolk gradient. *Dev. Biol.* **122**, 101-112.

den Elzen, N. and Pines, J. (2001). Cyclin A is destroyed in prometaphase and can delay chromosome alignment and anaphase. *J. Cell Biol.* **153**, 121-136.

Dworkin, M. B. and Dworkin-Rastl, E. (1991). Carbon metabolism in early amphibian embryos. *Trends Biochem. Sci.* **16**, 229-234.

Fagotto, F. (1995). Regulation of yolk degradation, or how to make sleepy lysosomes. *J. Cell Sci.* **108**, 3645-3647.

Fagotto, F. and Maxfield, F. R. (1994). Changes in yolk platelet pH during *Xenopus laevis* development correlate with yolk utilization. A quantitative confocal microscopy study. *J. Cell Sci.* **107**, 3325-3337.

Fischer, A., Dorresteijn, A. W. and Hoeger, U. (1996). Metabolism of oocyte construction and the generation of histospecificity in the cleaving egg. Lessons from nereid annelids. *Int. J. Dev. Biol.* **40**, 421-430.

Gerhart, J. C. (1980). Mechanisms regulating pattern formation in the amphibian egg and early embryo. In *Biological Regulation and Development, Vol. 2, Molecular Organization and Cell Function* (ed. R. F. Goldberger), pp. 133-316. New York: Plenum Press.

Getz, G. S. and Reardon, C. A. (2004). Paraoxonase, a cardioprotective enzyme: continuing issues. *Curr. Opin. Lipidology* **15**, 261-267.

Grant, B. and Hirsh, D. (1999). Receptor-mediated endocytosis in the *Caenorhabditis elegans* oocyte. *Mol. Biol. Cell* **10**, 4311-4326.

Grbac-Ivankovic, S., Antonijczuk, K., Varghese, A. H., Plowman, M. C., Antonijczuk, A., Korza, G., Ozols, J. and Sunderman, F. W., Jr (1994). Lipovitellin 2 beta is the 31 kD Ni(2+)-binding protein (pNiXb) in *Xenopus* oocytes and embryos. *Mol. Reprod. Dev.* **38**, 256-263.

Gurdon, J. B. and Wakefield, L. (1986). Microinjection of amphibian oocytes and eggs for the analysis of transcription. In *Microinjection and Organelle Transplantation Techniques* (ed. J. E. Celis, A. Graessmann and A. Loyter). London: Academic Press.

Hagedorn, H. H., Fallon, A. M. and Laufer, H. (1973). Vitellogenin synthesis by the fat body of the mosquito *Aedes aegypti*: evidence of transcriptional control. *Dev. Biol.* **31**, 285-294.

Hardcastle, Z. and Papalopulu, N. (2000). Distinct effects of XBF-1 in regulating the cell cycle inhibitor p27(XIC1) and imparting a neural fate. *Development* **127**, 1303-1314.

Harris, W. A. and Hartenstein, V. (1991). Neuronal determination without cell division in *Xenopus* embryos. *Neuron* **6**, 499-515.

Hausen, P. and Riebesell, M. (1991). *The Early Development of Xenopus laevis: An Atlas of the Histology*. Berlin: Springer-Verlag.

Hayakawa, H., Andoh, T. and Watanabe, T. (2006). Precursor structure of egg proteins in the coral Galaxea fascicularis. *Biochem. Biophys. Res. Commun.* **344**, 173-180.

Holland, L. J. and Wangh, L. J. (1987). Estrogen induction of a 45 kDa secreted protein coordinately with vitellogenin in *Xenopus* liver. *Mol. Cell. Endocrinol.* **49**, 63-73.

Holland, L. J., Suksang, C., Wall, A. A., Roberts, L. R., Moser, D. R. and Bhattacharya, A. (1992). A major estrogen-regulated protein secreted from the liver of *Xenopus laevis* is a member of the serpin superfamily. Nucleotide sequence of cDNA and hormonal induction of mRNA. *J. Biol. Chem.* **267**, 7053-7059.

Irving, J. A., Pike, R. N., Lesk, A. M. and Whisstock, J. C. (2000). Phylogeny of the serpin superfamily: implications of patterns of amino acid conservation for structure and function. *Genome Res.* **10**, 1845-1864.

Jacobsen, L., Hermann, M., Vieira, P. M., Schneider, W. J. and Nimpf, J. (1995). The chicken oocyte receptor for lipoprotein deposition recognizes alpha 2-macroglobulin. *J. Biol. Chem.* **270**, 6468-6475.

Jared, D. W., Dumont, J. N. and Wallace, R. A. (1973). Distribution of incorporated and synthesized protein among cell fractions of *Xenopus* oocytes. *Dev. Biol.* **35**, 19-28.
Karasaki, S. (1963). Studies on amphibian yolk. 5. Electron microscopic observations on the utilization of yolk platelets during embryogenesis. *J. Ultrastruct. Res.* **59**, 225-247.
Kimble, J. and Sharrock, W. J. (1983). Tissue-specific synthesis of yolk proteins in *Caenorhabditis elegans*. *Dev. Biol.* **96**, 189-196.
Komazaki, S. and Hiruma, T. (1999). Degradation of yolk platelets in the early amphibian embryo is regulated by fusion with late endosomes. *Dev. Growth Differ.* **41**, 173-181.
Komazaki, S., Tanaka, N. and Nakamura, H. (2002). Regional differences in yolk platelet degradation activity and in types of yolk platelets degraded during early amphibian embryogenesis. *Cells Tissues Organs* **172**, 13-20.
Kotyza, J., Varghese, A. H., Korza, G. and Sunderman, F. W., Jr (1998). Interactions of serine proteinases with pNiXa, a serpin of *Xenopus* oocytes and embryos. *Biochim. Biophys. Acta.* **1382**, 266-276.
Montorzi, M., Falchuk, K. H. and Vallee, B. L. (1995). Vitellogenin and lipovitellin: zinc proteins of *Xenopus laevis* oocytes. *Biochemistry* **34**, 10851-10858.
Neff, A. W., Wakahara, M., Jurand, A. and Malacinski, G. M. (1984). Experimental analyses of cytoplasmic rearrangements which follow fertilization and accompany symmetrization of inverted *Xenopus* eggs. *J. Embryol. Exp. Morphol.* **80**, 197-224.
Newport, J. and Kirschner, M. (1982). A major developmental transition in early *Xenopus* embryos: I. Characterization and timing of cellular changes at the midblastula stage. *Cell* **30**, 675-686.
Nieuwkoop, P. D. and Faber, J. (1994). *Normal Table of Xenopus laevis (Daudin)*, 2nd edn. New York: Garland Publishing.
Ohlendorf, D. H., Barbarash, G. R., Trout, A., Kent, C. and Banaszak, L. J. (1977). Lipid and polypeptide components of the crystalline yolk system from *Xenopus laevis*. *J. Biol. Chem.* **252**, 7992-8001.
Opresko, L., Wiley, H. S. and Wallace, R. A. (1980). Differential postendocytotic compartmentation in *Xenopus* oocytes is mediated by a specifically bound ligand. *Cell* **22**, 47-57.
Pierandrei-Amaldi, P., Campioni, N., Beccari, E., Bozzoni, I. and Amaldi, F. (1982). Expression of ribosomal-protein genes in *Xenopus laevis* development. *Cell* **30**, 163-171.
Richard-Parpaillon, L., Cosgrove, R. A., Devine, C., Vernon, A. E. and Philpott, A. (2004). G1/S phase cyclin-dependent kinase overexpression perturbs early development and delays tissue-specific differentiation in *Xenopus*. *Development* **131**, 2577-2586.
Robertson, N. (1978). Labilization of the superficial layer and reduction in size of yolk platelets during early development of *Xenopus laevis*. *Cell Differ.* **7**, 185-192.
Romano, M., Rosanova, P., Anteo, C. and Limatola, E. (2004). Vertebrate yolk proteins: a review. *Mol. Reprod. Dev.* **69**, 109-116.
Roth, T. F. and Porter, K. R. (1964). Yolk protein uptake in the oocyte of the mosquito *Aedes aegypti*. L. *J. Cell Biol.* **20**, 313-332.
Saka, Y. and Smith, J. C. (2001). Spatial and temporal patterns of cell division during early *Xenopus* embryogenesis. *Dev. Biol.* **229**, 307-318.
Sambrook, J. and Russell, D. W. (2001). *Molecular Cloning: A Laboratory Manual*. Cold Spring Harbor, NY: Cold Spring Harbor Laboratory Press.
Schneider, W. J. (1996). Vitellogenin receptors: oocyte-specific members of the low-density lipoprotein receptor supergene family. *Int. Rev. Cytol.* **166**, 103-137.
Selchow, A. and Winklbauer, R. (1997). Structure and cytoskeletal organization of migratory mesoderm cells from the *Xenopus* gastrula. *Cell Motil. Cytoskeleton* **36**, 12-29.
Selman, G. G. and Pawsey, G. J. (1965). The utilization of yolk platelets by tissues of *Xenopus* embryos studied by a safranin staining method. *J. Embryol. Exp. Morphol.* **14**, 191-212.
Sive, H. L., Grainger, R. M. and Harland, R. M. (2000). *Early Development of Xenopus laevis: A Laboratory Manual*. Cold Spring Harbor, NY: Cold Spring Harbor Laboratory Press.
Smolenaars, M. M., Madsen, O., Rodenburg, K. W. and Van der Horst, D. J. (2007). Molecular diversity and evolution of the large lipid transfer protein superfamily. *J. Lipid Res.* **48**, 489-502.
Sunderman, F. W., Jr, Varghese, A. H., Kroftova, O. S., Grbac-Ivankovic, S., Kotyza, J., Datta, A. K., Davis, M., Bal, W. and Kasprzak, K. S. (1996). Characterization of pNiXa, a serpin of *Xenopus laevis* oocytes and embryos, and its histidine-rich, Ni(II)-binding domain. *Mol. Reprod. Dev.* **44**, 507-524.
Thompson, J. R. and Banaszak, L. J. (2002). Lipid-protein interactions in lipovitellin. *Biochemistry* **41**, 9398-9409.
Tuft, P. H. (1962). The uptake and distribution of water in the embryo of *Xenopus laevis* (Daudin). *J. Exp. Biol.* **39**, 1-19.
Wahli, W., Dawid, I. B., Ryffel, G. U. and Weber, R. (1981). Vitellogenesis and the vitellogenin gene family. *Science* **212**, 298-304.
Wallace, R. A. and Karasaki, S. (1963). Studies on amphibian yolk. 2. The isolation of yolk platelets from the eggs of *Rana pipiens*. *J. Cell Biol.* **18**, 153-166.
Wiley, H. S. and Wallace, R. A. (1981). The structure of vitellogenin: multiple vitellogenins in *Xenopus laevis* give rise to multiple forms of the yolk proteins. *J. Biol. Chem.* **256**, 8626-8634.

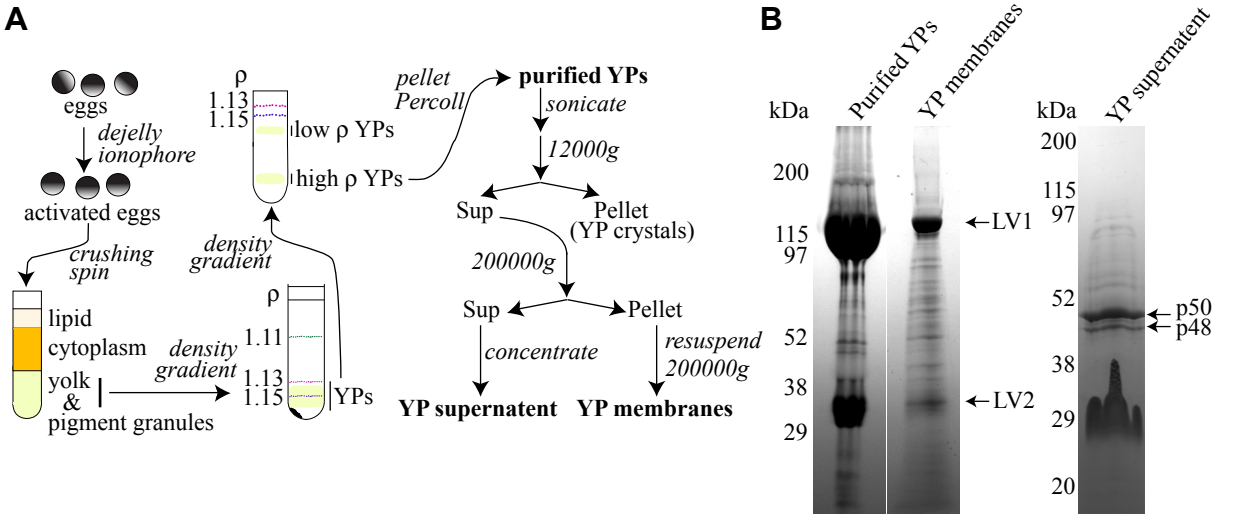
A
eggs
dejelly
ionophore
activated eggs
crushing
spin
lipid
cytoplasm
yolk
&
pigment granules
density
gradient
ρ
1.11
1.13
1.15
YPs
density
gradient
ρ
1.13
1.15
low ρ YPs
high ρ YPs
pellet
Percoll
purified YPs
sonicate
12000g
Sup
Pellet
(YP crystals)
200000g
Sup
Pellet
concentrate
resuspend
200000g
YP supernatent
YP membranes
B
kDa
Purified YPs
YP membranes
200
115
97
52
38
29
LV1
LV2
kDa
YP supernatent
200
115
97
52
38
29
20
p50
p48

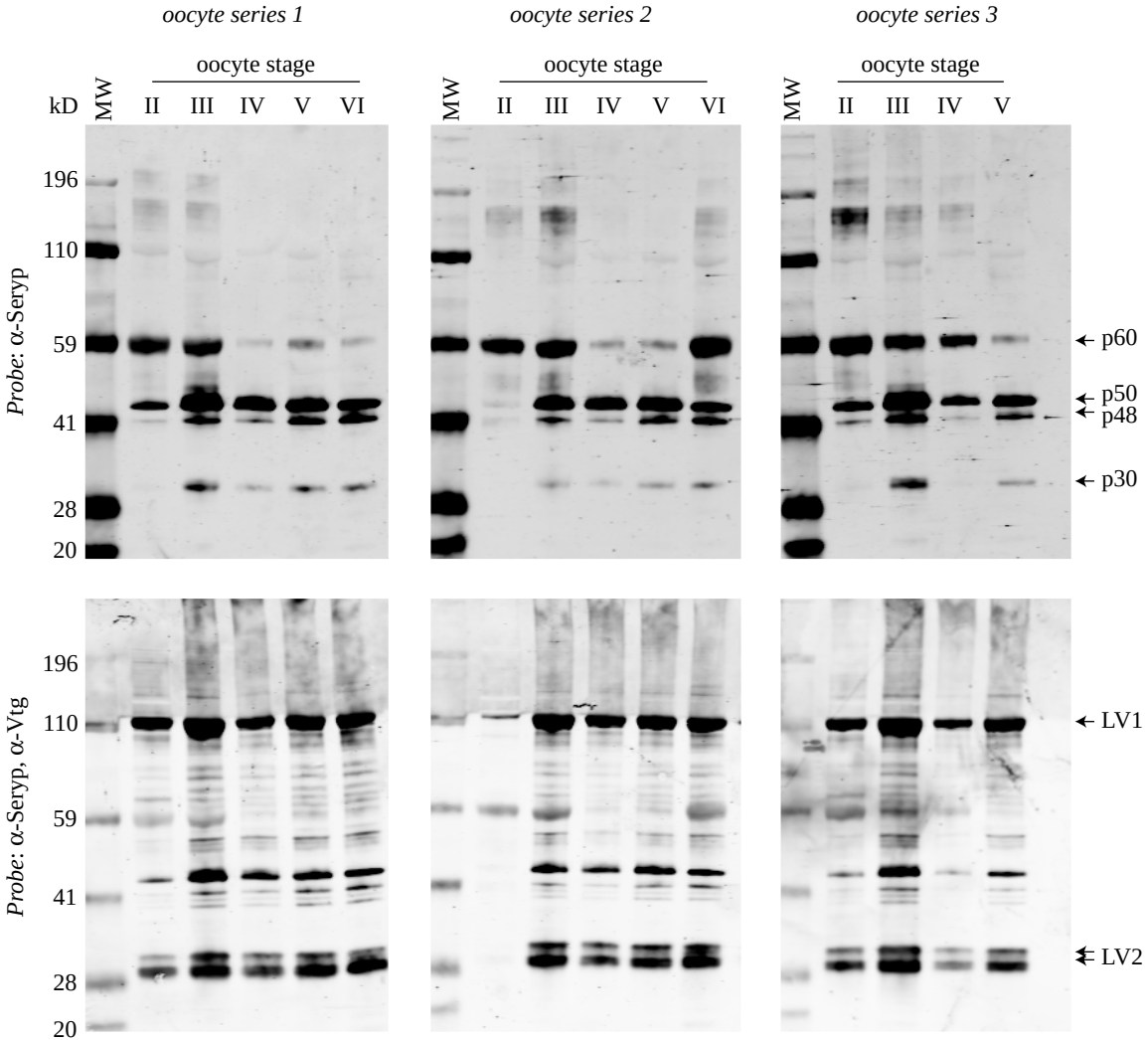
oocyte series 1
oocyte series 2
oocyte series 3
oocyte stage
kD
MW
II
III
IV
V
VI
196
110
59
41
28
20
Probe: α-Seryp
p60
p50
p48
p30
Probe: α-Seryp, α-Vtg
LV1
LV2

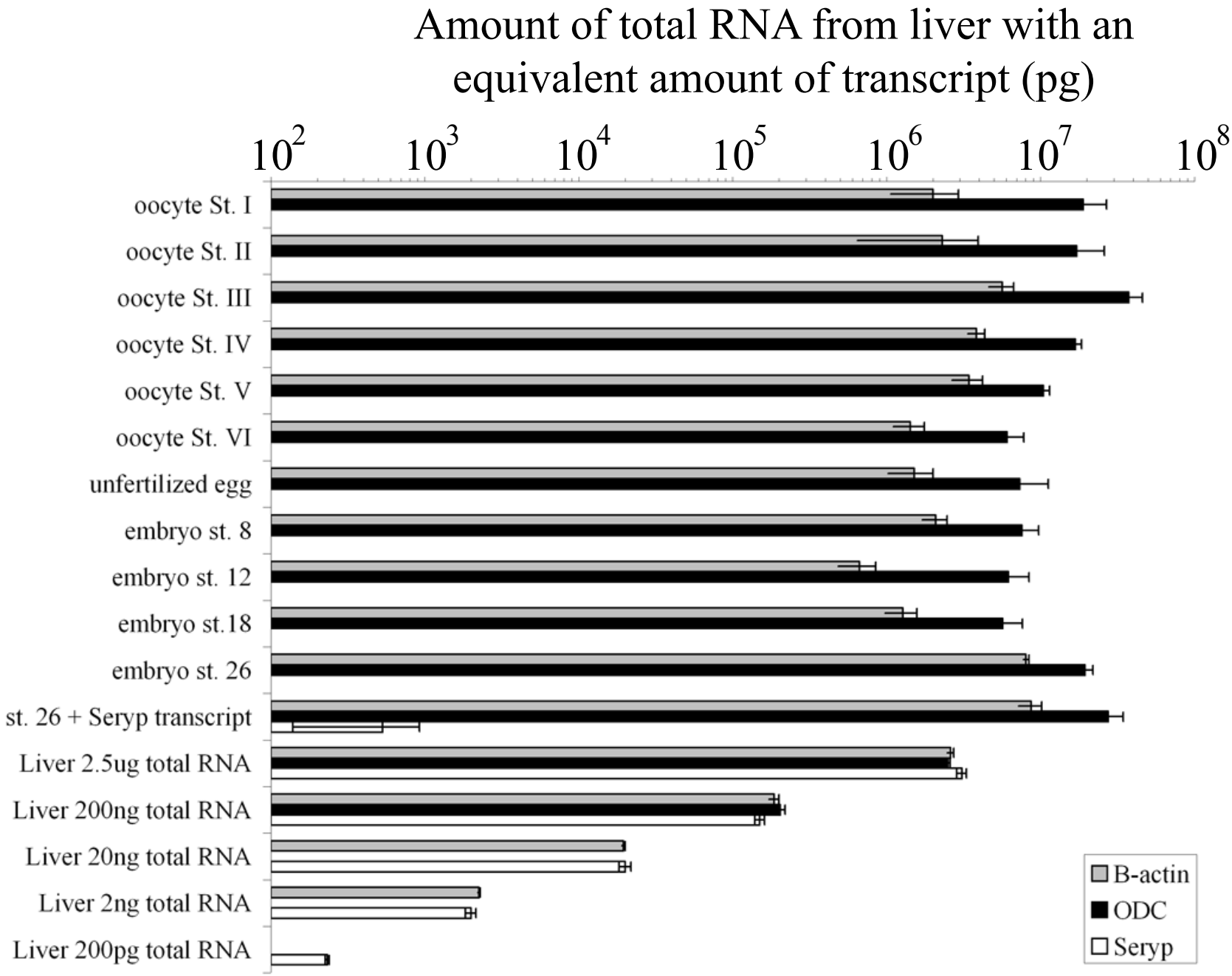
Amount of total RNA from liver with an equivalent amount of transcript (pg)
10^2
10^3
10^4
10^5
10^6
10^7
10^8
oocyte St. I
oocyte St. II
oocyte St. III
oocyte St. IV
oocyte St. V
oocyte St. VI
unfertilized egg
embryo st. 8
embryo st. 12
embryo st.18
embryo st. 26
st. 26 + Seryp transcript
Liver 2.5ug total RNA
Liver 200ng total RNA
Liver 20ng total RNA
Liver 2ng total RNA
Liver 200pg total RNA
B-actin
ODC
Seryp

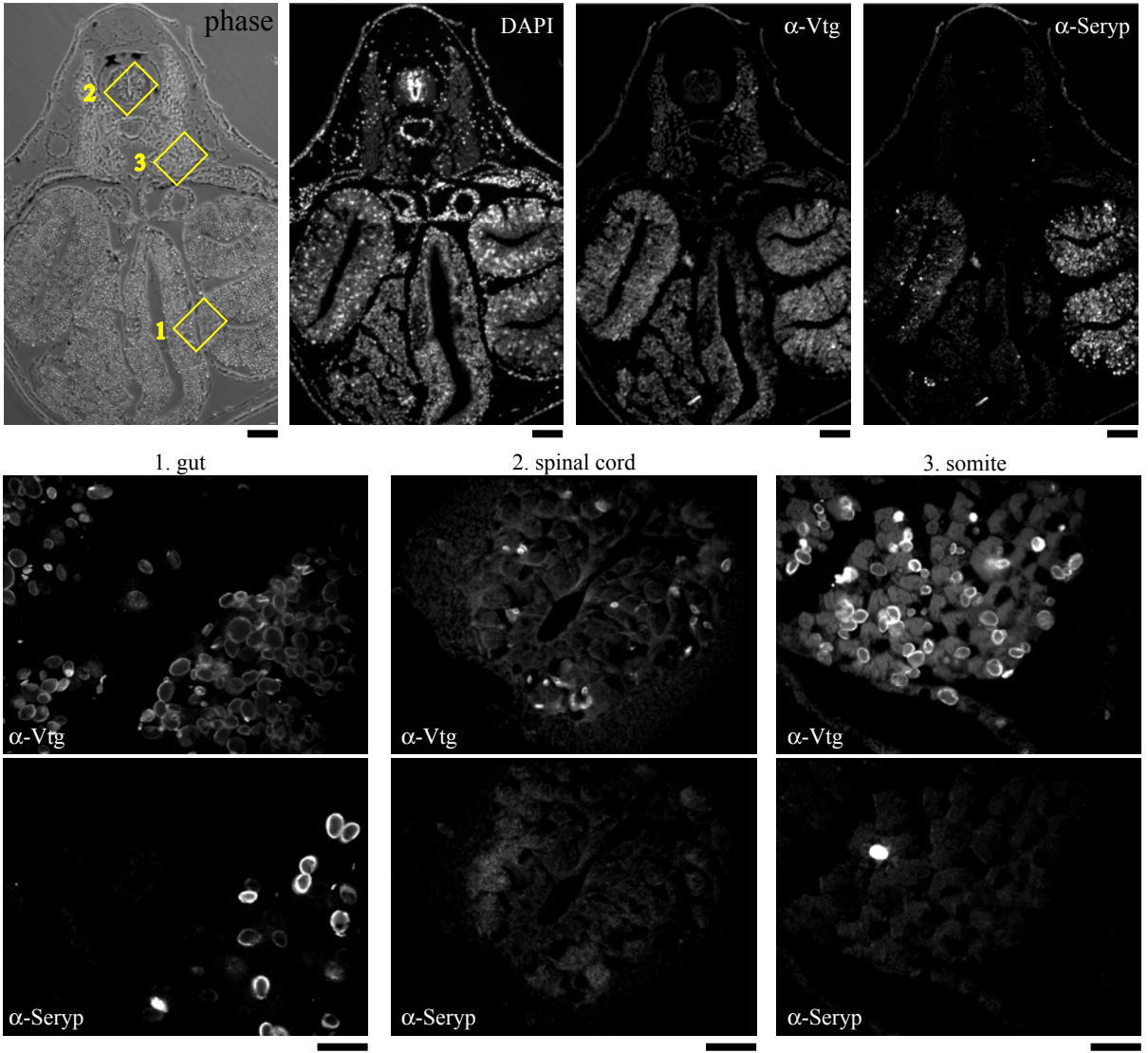
phase
DAPI
α-Vtg
α-Seryp
2
3
1
1. gut
2. spinal cord
3. somite
α-Vtg
α-Vtg
α-Vtg
α-Seryp
α-Seryp
α-Seryp

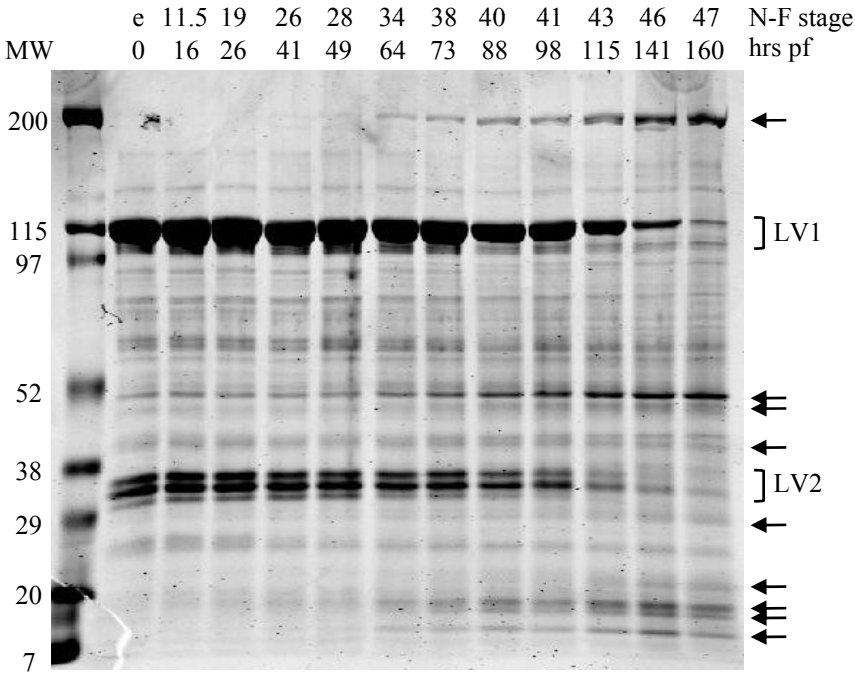
e 11.5 19 26 28 34 38 40 41 43 46 47 N-F stage
MW 0 16 26 41 49 64 73 88 98 115 141 160 hrs pf
200
115
97
52
38
29
20
7
LV1
LV2

Table S1. Proteins identified in the membrane and supernatant fractions of purified yolk platelets

Identified proteins	GI number	YP membranes or supernatant?	Description
Yolk platelets			
Vitellogenin A2	gi|4388696	Both	Major yolk protein, estrogen inducible (liver)
Vitellogenin B1	gi|33563034	Both	Major yolk protein, estrogen inducible (liver)
Plasma			
Ep45	gi|259142	Both	Protein found in *X. laevis* plasma and eggs, estrogen inducible (liver)
MGC64276	gi|32766455	YP membranes	Homolog of human complement component C9
Pon1-prov	gi|28422437	YP membranes	Homolog of paraoxonase, hydrolyzes oxidized lipids in LDL
MGC82702	gi|49256138	YP supernatant	Homolog of alpha globin, subunit of hemoglobin
LOC448844	gi|51895923	YP supernatant	Serum albumin
Lysosome			
LOC432087	gi|71051360	YP membranes	Predicted alpha-L-1 fucosidase
Manba-prov	gi|50417768	YP supernatant	Predicted beta-mannosidase
MGC64382, dipeptidyl-peptidase IV	gi|111185523, gi|147907306	YP supernatant	Dipeptidyl-peptidase IV, serine protease, hydrolyzes N-terminus dipeptides
LOC446948	gi|71681246	YP supernatant	Predicted galactocerebrosidase
Ctsc-prov	gi|33417162	YP supernatant	Dipeptidyl aminopeptidase I, cysteine protease, hydrolyzes N-terminus dipeptides
Endoplasmic reticulum			
LOC495169	gi|54038199	YP membranes	Homolog of human ERp72, a protein disulfide isomerase
Grp58-prov	gi|28302197	Both	Homolog of human ERp57, a protein disulfide isomerase, associates with ApoB100
P4hb	gi|28436918	Both	Homolog of human PDI, a protein disulfide isomerase
MGC79068	gi|50418205	YP membranes	Homolog of human P5, a protein disulfide isomerase
MGC52808, MGC52894	gi|28277278, gi|28175644	YP membranes	Predicted Ribophorin I
MGC53764	gi|28436786	YP membranes	Predicted Ribophorin II
MGC84282, LOC495100	gi|49522162, gi|54038026	YP membranes	Homolog of human ERLIN2, prohibitin family member
MGC68448, heat shock protein gp96	gi|37805387, gi|148223467	YP supernatant	Predicted Hsp90 chaperone
Hspa5	gi|27370850	Both	Nearly identical to *X. laevis* BiP, Hsp70 chaperone
Mitochondria			
MGC82638	gi|49256557	YP membranes	Predicted hydroxyacyl-Coenzyme A dehydrogenase
Atp5b	gi|28436792	YP membranes	Predicted ATP synthase, mitochondrial F1 complex, beta subunit precursor
Atp5a1	gi|32766606	YP membranes	Predicted ATP synthase, mitochondrial F1 complex, alpha subunit
MGC82361, MGC82400, MGC82361	gi|47682284, gi|46329495, gi|47682284	YP membranes	Predicted ATP synthase, mitochondrial F0 complex, subunit d
Thiolase-prov	gi|28280033	YP membranes	Predicted hydroxyacyl-Coenzyme A dehydrogenase
Mitochondrial malate dehydrogenase	gi|50882324	YP membranes	Mitochondrial malate dehydrogenase 2a
MGC114756	gi|62826006	YP membranes	Predicted voltage-dependent anion-selective channel protein
MGC79025	gi|50417418	YP membranes	Predicted Prohibitin 2
Hspd1, MGC53106	gi|47938737, gi|28436902	Both	Predicted Hsp60 chaperone
Location not classified			
MGC68676	gi|37747702	YP supernatant	Predicted phospholipase D3, involved in signalling pathways
MGC82953	gi|148228657	YP supernatant	Predicted VAT1, a vesicle amine transport protein
MGC81039	gi|46249838	YP membranes	Homolog of yeast Yop1, binds to Rab proteins
Rheb-prov	gi|27695152	YP membranes	Predicted Rheb, GTPase, growth regulator upstream of TOR
MGC64421	gi|32450604	YP membranes	Homolog of human thrombin inhibitor, an intracellular serpin
Cytoplasm			
MGC53952	gi|28374367	Both	Nearly identical to *X. laevis* Hsc70, constitutively expressed Hsp70 protein
LOC443576	gi|48734658	YP membranes	Predicted inosine monophosphate synthase, de novo purine biosynthesis
Pgm2-prov	gi|27881782	YP membranes	Predicted phosphoglucomutase, glycogen metabolism
MGC69114	gi|33585659	YP membranes	Predicted transketolase, pentose phosphate pathway
Cct3-prov	gi|29477224	YP membranes	Predicted subunit of CCT chaperonin

Cct8-prov	gi|27924345	YP membranes	Predicted subunit of CCT chaperonin
PKM2	gi|51258124	YP membranes	Predicted pyruvate kinase, glycolysis
MGC53997	gi|27695233	YP membranes	Predicted beta-tubulin
Eno1-prov	gi|32450571	YP membranes	Predicted enolase, glycolysis
MGC64329	gi|32484263	YP membranes	Predicted elongation factor 1 gamma
Actin	gi|1334642	YP membranes	Predicted beta-actin
MGC53030	gi|28302293	YP membranes	Predicted fructose bisphosphate aldolase
Ckb-prov	gi|27503418	YP membranes	Predicted creatine kinase
Gapd-prov	gi|27882192	YP membranes	Predicted glyceraldehyde 3-phosphate dehydrogenase, glycolysis
NM23	gi|1655706	YP membranes	Nucleoside diphosphate kinase
Cofilin-1, Cofilin-2	gi|148232082, gi|1168995	YP membranes	Actin regulation
MGC82306	gi|46329492	YP membranes	Predicted 40S ribosomal protein S18
Rpl27-prov	gi|34193964	YP membranes	Predicted 60S ribosomal protein L27
Ferritin heavy chain	gi|33331485	YP membranes	Forms iron storage complexes
14-3-3 zeta, Ywhaz-prov	gi|1360640, gi|27370992	YP membranes	14-3-3 protein
Ppib-prov, LOC495270	gi|32484306, gi|54261578	YP membranes	Predicted peptidylprolyl isomerase B

The GI number of each identification by the Mascot software and the associated protein name are listed. If the protein has not been assigned a function in *X. laevis*, as in the great majority of cases, BLAST searches were used to assign homologs and predicted functions. When highly similar (>95% amino acid identity) proteins were identified by mass spectrometry; they were assumed to be pseudo-alleles and are listed in the same row, separated by a comma.

Table S2. The percentage of yolk platelets lacking Seryp (Seryp$^-$) was determined in the listed tissues at seven developmental Nieuwkoop-Faber (NF) stages

Tissue	Time pf (hour)	NF stage	*n*	Average Seryp$^-$ (%)	s.d. Seryp$^-$ (%)
Unactivated egg	**0**	**egg**			
Animal pole			3	2.1	2.1
Marginal zone			3	1.2	2.0
Vegetal pole			3	0.5	0.5
Blastula	**8.5**	**9**			
Animal pole			3	1.5	0.3
Marginal zone			3	1.5	1.4
Vegetal pole			3	1.0	1.0
Gastrula	**20.5**	**12**			
Neurectoderm			3	7.0	3.0
Epidermal ectoderm			3	5.8	3.0
Dorsal lip			3	5.0	1.9
Archentron roof			3	0.3	0.5
Deep endoderm			3	1.5	0.7
Early neurula	**23**	**14**			
Anterior neural plate			3	22.1	1.3
Neural plate (mid-body)			3	17.8	1.5
Epidermal ectoderm			3	17.4	4.5
Notochord			3	13.9	3.8
Somitogenic mesoderm			3	11.6	3.7
Archentron roof			3	6.1	3.9
Deep endoderm			3	3.7	3.5
Late neurula	**27**	**18**			
Prosencephalon			3	29.7	4.1
Neural groove (mid-body)			3	31.8	6.5
Cement gland anlage			3	29.3	3.4
Epidermal ectoderm			3	22.6	2.6
Notochord			3	15.3	0.1
Somitogenic mesoderm			3	14.1	3.8
Archentron roof			4	8.0	1.8
Deep endoderm			3	3.1	2.9
Early tailbud	**30**	**21**			
Eye anlage			5	46.9	9.1
Prosencephalon			5	41.0	8.9
Neural tube (mid-body)			3	29.3	10.8
Cement gland anlage			4	35.8	6.3
Epidermis			4	25.0	6.1
Notochord			4	24.3	6.7
Somite			4	23.4	10.6
Archentron roof			4	7.7	5.6
Deep endoderm			4	3.2	1.8
Tailbud	**47**	**27**			
Eye vesicle			3	82.1	11.8
Prosencephalon			3	61.2	13.9
Otic vesicle			3	57.6	6.5
Lens placode			3	64.3	5.2
Cement gland			3	72.7	19.4
Epidermis			3	44.8	4.2
Notochord			3	55.8	14.4
Somites			4	53.2	19.4
Heart anlage			3	40.9	11.0
Tailbud tip			3	47.5	4.7
Arch endoderm epithelium			4	30.7	10.4
Oral endoderm epithelium			4	23.2	9.5
Deep endoderm			3	9.3	1.0

The number (*n*) of measurements is noted; in all tissues at all stages, at least three measurements were made on embryos derived from different female frogs and so are genetically independent. In most cases, embryos were derived from different males as well. The time post-fertilization (pf) is noted and corresponds to the majority of measurements (76%) made on embryos that were reared at 22°C. The remaining measurements (22%) were made on embryos reared at 18°C, except for three measurements made on one stage 9 embryo that was reared at 13°C. We noted no obvious effects of temperature on Seryp$^-$ (%).